Arrive and wait: inactive bacterial taxa contribute to perceived soil microbiome resilience after a multidecadal press disturbance

Samuel E. Barnett (barne424@msu.edu)[1], Ashley Shade (ashley.shade@cnrs.fr)[2*]

[1]Department of Microbiology and Molecular Genetics, Michigan State University, East Lansing, MI 48824, USA

[2] Universite Claude Bernard Lyon 1; CNRS, UMR 5557 Écologie Microbienne, 16 rue Dubois 69622 Villeurbanne Cedex, FRANCE

Running title: Mechanisms of soil microbiome resilience

Keywords: Microbial ecology, soil, resilience, fire, dormancy, high-throughput sequencing, temporal dynamics, disturbance ecology, community ecology, interannual

Type of Article: Letter

No. abstract words: 150

No. main text words: 4997

No. references: 64

No. figures: 6

Corresponding author: Ashley Shade

UMR5557 - Ecologie Microbienne Lyon

Université Claude Bernard Lyon 1
Bât. Mendel, 5eme étage
16 Rue Dubois
69622 Villeurbanne cedex, FRANCE
+33472431377
ashley.shade@cnrs.fr

Statement of authorship:

AS conceptualized the research, AS and SB collected soil samples at the research site (investigation), SB performed laboratory work and conducted formal analysis (investigation), SB performed data curation, SB wrote the original draft manuscript, SB and AS contributed to review and editing of the manuscript, SB performed data visualization, and AS provided supervision, administration, and funding acquisition.

Data accessibility statement:

Raw sequences are available on the NCBI short read archive BioProject PRJNA973689. Representative OTU sequences in FASTA format, along with metadata, OTU table, taxonomy table, and phylogenetic tree, all in a phyloseq object, are available through figshare DOI: 10.6084/m9.figshare.23060354. Sequence processing and analysis code are available through GitHub at https://github.com/ShadeLab/Centralia_RNA_DNA_multiyear.

Abstract

Long-term (press) disturbances like the climate crisis and other anthropogenic pressures are fundamentally altering ecosystems and their functions. Many critical ecosystem functions, such as biogeochemical cycling, are facilitated by microbial communities. Understanding the functional consequences of microbiome responses to press disturbances requires ongoing observations of the active populations that contribute functions. This study leverages a 7-year time series of a 60-year-old coal seam fire (Centralia, Pennsylvania, USA) to examine the resilience of soil bacterial microbiomes to a press disturbance. Using 16S rRNA and 16S rRNA gene amplicon sequencing, we assessed the interannual dynamics of the active subset and the "whole" bacterial community. Contrary to our hypothesis, the whole communities demonstrated greater resilience than active subsets, suggesting that inactive members contributed to overall resilience. Thus, in addition to selection mechanisms of active populations, perceived microbiome resilience is also supported by mechanisms of dispersal, persistence, and revival from the local dormant pool.

Introduction

The climate crisis and anthropogenic pressure on the environment fundamentally change ecosystems and their functions. Soil microbial communities are vital to ecosystem functioning, filling important roles in biogeochemical cycling (Madsen 2011) and plant health (Mendes *et al.* 2013; Turner *et al.* 2013), among other ecosystem services. Thus, understanding the responses and functional consequences of microbial communities to severe disturbances is essential for advancing a holistic understanding of climate change and anthropogenic pressures' impact on the natural world.

Community stability can be defined as the interplay between resistance (*i.e.,* the degree to which the community remains unchanged during a disturbance event) and resilience (*i.e., engineering resilience* (Holling 1996) or the rate at which the community returns to a pre-disturbance state) (Pimm 1984; Shade *et al.* 2012; Griffiths & Philippot 2013; Philippot *et al.* 2021). Microbial community resistance and resilience can vary substantially across soils and disturbances (Griffiths & Philippot 2013). The duration of a disturbance event, whether it is a pulse (*i.e.,* a discrete, short-term event) or press (*i.e.,* a long-term, continuous event), and whether the disturbance is compounded, may differentially affect the stability of the affected microbial community (Shade *et al.* 2012; Philippot *et al.* 2021). In light of the long-term environmental impacts of human activities and climate change across broad ecological scales, ongoing observations of microbial community dynamics to press disturbances, particularly during recovery, may illuminate the mechanisms behind community resilience to important environmental pressures.

Microbial communities tend to have low resistance to disturbances (Shade *et al.* 2012). However, the rate and degree of resilience of these communities can vary widely. The perceived

variability in resilience may be due to complex, interacting, and poorly understood ecological and evolutionary mechanisms (Shade *et al.* 2012; Griffiths & Philippot 2013; Shade 2023), including the interplay of speciation, selection, and dispersal assembly processes (Vellend 2010; Nemergut *et al.* 2013). Quantifications of microbiome resilience may also be complicated by the substantial pool of dormant microorganisms that persists in many environmental systems, but especially in soils (Aanderud *et al.* 2015). Dormancy is a reversible state of extremely low metabolism that can allow bacteria to survive under poor conditions or during disturbance (Jones & Lennon 2010; Lennon & Jones 2011; Kearns & Shade 2018). Some dormant bacterial cells can remain viable for extended periods, and some can be selectively revived given conducive growth conditions (Jones & Lennon 2010; Lennon & Jones 2011). Because ecosystem response to disturbance reflects the functions of active microbiome members (Allison & Martiny 2008; Shade *et al.* 2012), it is important to account for the dynamics of active members to develop more direct predictors of ecosystem resilience and functional recovery.

The six-decade-old coal mine fire in Centralia, Pennsylvania, USA, provides a unique case study to examine the resilience of soil microbial communities to an intense, long-term heat disturbance (Shade 2018). The surface soils above the active fires are continuously hotter than ambient soil temperatures and coal combustion products percolate through the soil and open vents in the ground, altering soil chemistry at the surface (Tobin-Janzen *et al.* 2005; Janzen & Tobin-Janzen 2008; Elick 2011). The gradual advancement of the fire along the coal seams allows for direct comparisons across a gradient of disturbance intensities (*i.e.,* soil temperature) and across fire-affected, decades-old recovered, and unaffected reference soils, all within an area encompassing less than 0.35 km^2 (Shade 2018). Furthermore, as disturbance intensity changes

102 over time within a site, community changes can be tracked and understood in the context of the
103 dynamic warming and cooling that define this press disturbance.
104 The overarching goal of this study was to understand the ecological mechanisms that
105 support soil microbiome resilience. Our previous work in Centralia revealed that soil bacterial
106 communities had a high capacity to recover from warming (within approximately 8-10 years)
107 despite their multi-year exposure to the disturbance (Lee *et al.* 2017; Sorensen & Shade 2020).
108 Advancing, we conducted a 7-year study that delineated the "whole" bacterial communities from
109 the subset of their active members to understand the contributions of dormancy as a potential
110 mechanism of resilience. Samples were annually collected from established Centralia sites
111 representing fire-affected, recovered, and reference soils (Fig. 1A, Table S1). Whole bacterial
112 communities were assessed using 16S rRNA gene amplicons, which include contributions of
113 active, dormant, and recently deceased cells. The active subset of the whole community was
114 determined by filtering the dataset to include only the taxa that met a conservative, population-
115 level activity criterion based on their 16S rRNA to 16S rRNA gene ratios (Blagodatskaya &
116 Kuzyakov 2013; Bowsher *et al.* 2019). We applied several specific methods to quantify the
117 microbiome recovery of the whole community and their active subsets relative to the disturbance
118 intensity, particularly time-lag and trajectory analysis (Beisner *et al.* 2003; Lamothe *et al.* 2019).
119 Building from previous findings (Lee *et al.* 2017; Kearns & Shade 2018), we hypothesized that
120 the microbiome resilience is largely attributable to directional changes in the active populations,
121 indicative of environmental selection driving community turnover as the soils cool.
122 This work illuminates the resilience of the often overlooked, inactive part of the
123 community that is nonetheless viable and can become interactive. By considering the dormant
124 microbial pool, this work indicates the need for careful consideration of how recovery of

125 microbiome structure (which taxa are detected and in what relative contributions) influences
126 microbial community functional recovery after disturbance. Thus, this study advances
127 understanding of the complex and interacting ecological mechanisms that drive microbial
128 community responses to disturbance.
129

130 **Materials and Methods**

131 *Study site, soil collection, and processing*

132 Centralia, Pennsylvania, overlies an anthracite seam that has been burning constantly
133 since 1962 (Elick 2011). Heat and combustion gasses from the fire about 46m deep make their
134 way to the surface, increasing surface soil temperatures and producing steam vents (Elick 2011).
135 Nineteen sites were selected based on previous experiments (Lee *et al.* 2017; Kearns & Shade
136 2018), including three reference, four recovered, and 12 fire-affected (supplemental materials;
137 Table S1). Soils were collected from each site from 2015 to 2021 in the beginning of October. 20
138 cm deep soil cores were collected as previously described (Lee *et al.* 2017; Kearns & Shade
139 2018) with sterilized PVC soil corer or trowel, sieved to 4 mm, homogenized, and aliquots for
140 nucleotide extraction were flash frozen in liquid N_2 (detailed in supplemental materials). Soil and
141 air temperatures were collected with an electronic thermometer, and CO_2 venting was measured
142 using an EGM-5 portable CO_2 gas analyzer (PP Systems, Amesbury, USA). Daily soil
143 temperatures were monitored throughout the year at five sites (Table S1) using HOBO 64K
144 pendant Temperature data loggers (UA-001-64; ONSET, Bourne USA). Soil moisture was
145 measured gravimetrically, and soil chemistry analysis was performed by the Soil and Plant
146 Nutrition Lab at Michigan State University (East Lansing, USA;
147 https://www.canr.msu.edu/spnl).

148

149 *DNA/RNA extraction and processing*

150 DNA and RNA were coextracted from 0.25 g of soil following a published phenol-
151 chloroform protocol (Griffiths *et al.* 2000), with the alternate use of 0.1 mm zirconium bead
152 containing BeadBug homogenizer tubes (#Z763764; Benchmark Scientific, Sayreville USA) for
153 bead beating. Both positive (*i.e.,* mock bacterial and fungal community (Colovas *et al.* 2022))
154 and negative (*i.e.,* nuclease-free water) nucleotide extraction controls were included for each
155 batch of nucleic acid extraction, and all controls were processed along with samples. DNA and
156 RNA aliquots were processed as previously described (Lee *et al.* 2017; Sorensen & Shade 2020)
157 and detailed in supplemental materials. To generate cDNA from RNA aliquots, DNA was
158 degraded using the TURBO DNA-free kit (#AM1907; Invitrogen, Waltham USA) following the
159 rigorous DNase treatment protocol for the RNA aliquot and RNA was reverse transcribed using
160 the SuperScript III Reverse Transcriptase kit (#18080093; Invitrogen) following the standard
161 protocol. Illumina MiSeq V4 region 16S rRNA gene amplification and sequencing of DNA and
162 cDNA were performed by the Genomics Core Research Technology Support Facility at
163 Michigan State University (East Lansing, MI, USA) following standard protocols as detailed in
164 supplemental materials. Triplicate sequencing runs were performed for both DNA libraries,
165 while single runs were performed for both RNA libraries. As detailed in supplemental materials,
166 16S rRNA gene counts in undiluted DNA extracts were quantified with qPCR to proxy overall
167 Bacterial and Archaeal community sizes across the disturbance intensity gradient.

168

169 *Sequence processing*

170 Sequence processing was performed using standard pipelines for amplicon sequencing as
171 previously described with custom scripts (Barnett *et al.* 2020) and detailed in supplemental
172 materials. We defined bacterial OTUs based on 16S rRNA gene sequence clusters at 97%
173 sequence identity, including DNA and RNA sequence sets. OTUs were used rather than ASVs to
174 avoid the potential artificial splitting of bacterial populations into multiple clusters (Glassman &
175 Martiny 2018; Schloss 2021) and to account for potential errors that could propagate among the
176 RNA amplicons due to the additional amplification required for reverse transcription.
177
178 *Statistical analyses.*
179 All statistical analyses were conducted using R (version 4.1.1) (R Core Team 2018). Due
180 to the repeated measures study design, we utilized linear mixed effects (LME) models from
181 package nlme (Pinheiro *et al.* 2020) to compare community, soil, and experimental features. In
182 all LME models, the site was the random effect. The Benjamini-Hochberg procedure was used
183 for all *post hoc* tests to adjust p-values for multiple comparisons. Change in soil temperature and
184 pH over time was examined within fire classifications with LME models. Differences in soil pH
185 across fire classifications were tested using ANOVA and post hoc Tukey's.
186 OTU counts from triplicate libraries were summed for DNA samples. Samples with less
187 than 100,000 reads were removed because these were clear outliers regarding sequence output,
188 suggesting low quality. Sites with less than three years of adequate DNA sequencing were
189 removed, and the resulting OTU table was rarefied to 161,171 reads and used for the whole
190 community analysis. To construct an OTU table for the active community, DNA samples
191 without a corresponding RNA sample after quality filtering and sites with less than three years of
192 paired DNA and RNA samples were removed, and the resulting OTU table was rarefied to

193 100,491 reads. OTUs found in an RNA sample but not the corresponding DNA sample (*i.e.,*
194 phantom OTUs, Fig. S1, supplemental material) were given a count of 1 in the DNA sample
195 (Blagodatskaya & Kuzyakov 2013; Bowsher *et al.* 2019). OTUs with an RNA: DNA ratio ≥ 1 in
196 each paired RNA and DNA sample were then defined as active (Blagodatskaya & Kuzyakov
197 2013; Bowsher *et al.* 2019). Analysis of the active community subset used the OTU tables from
198 the filtered DNA samples to only include active OTUs (*i.e.,* zero count wherever DNA and
199 cDNA count was zero or RNA: DNA ratio was < 1). Critically, DNA relative abundances (not
200 cDNA relative abundances) were used to determine active taxon dynamics, as the relativized
201 abundances of 16S rRNA are not indicative of population abundances due to the known
202 individual- and population-level heterogeneity in gene regulation, ribosomal gene copy number,
203 post-translational modification, ribosome stability, etc. (Blazewicz *et al.* 2013).
204 Alpha diversity was measured as Faith's phylogenetic diversity index (PD). Change in
205 PD over time within fire classifications and across soil temperature regardless of fire
206 classification was examined with LME models. Beta diversity was measured using abundance-
207 weighted UniFrac distance calculated with package phyloseq (McMurdie & Holmes 2013).
208 Variation in community structure across fire classification, sampling year, and their interaction
209 was performed using PERMANOVA blocked by site ID. *Post hoc* analysis of variation in
210 community structure across fire classifications within each year or across years within each fire
211 class was also performed using PERMANOVA blocked by site ID. Variation in community
212 structure explained by edaphic factors and temperature was examined using a constrained
213 correspondence analysis with package phyloseq. Selection of edaphic factors included in the
214 final models was accomplished with function ordistep from the vegan package (Oksanen *et al.*
215 2018) with the initial full model incorporating soil temperature, CO_2 emission, pH, percent soil

organic matter, and phosphate, potassium, calcium, magnesium, iron, nitrate, ammonium, sulfate, and arsenic concentrations.

We used two methods to assess community change over time. First, time-lag analysis measures the distance between communities within a site over increasing time-steps. The shape, particularly the slope, of the relationship between community distance and time-lag can indicate directional shifts in communities during recovery (Lamothe *et al.* 2019). Time-lag analysis was performed separately for each fire classification using LME models. Abundance-weighted UniFrac distance across time points within a site was the response variable, and the square root of time point difference was the fixed effect. Slopes of time-lag linear regressions for each site were then regressed to the maximum soil temperature at each site, regardless of fire classification, using a linear model. Second, community trajectory analyses measure directionality in community structure over time, which can indicate community recovery (Lamothe *et al.* 2019). Trajectory directionality was calculated using package ecotraj (De Cáceres *et al.* 2019; Sturbois *et al.* 2021) and was compared across fire classifications using a Kruskall-Wallis test and *post hoc* pairwise Dunn's tests. Trajectory directionality was also regressed to maximum soil temperature at each site, regardless of fire classification, using a linear model. To further assess whether the bacterial communities were becoming more like the undisturbed reference communities as soils cooled, we tested whether the distance in community structure between disturbed soils (*i.e.,* fire-affected and recovered soils) and reference soils within years was associated with time or disturbed soil temperature. We used LME models to compare the mean abundance-weighted UniFrac distance between the disturbed site and all three references, paired by timepoint, to year or soil core temperature.

238 We calculated the percentage of the Bray-Curtis dissimilarity within each site attributed
239 to active taxa using previously described methods (Shade *et al.* 2014), see Supplemental
240 Methods. To examine the influence of OTUs that become inactive or newly active over time, we
241 separately analyzed OTUs active in the first timepoint of each timepoint pair (*e.g.,* 2016 when
242 comparing 2016 to 2020) and in the second timepoint of each pair (*e.g.,* 2020 when comparing
243 2016 to 2020). The percentage of the Bray-Curtis dissimilarity attributed to active taxa was
244 compared across fire classifications using Kruskall-Wallis and *post hoc* pairwise Dunn's tests
245 and across time differences between samplings within each fire class using LME models.
246 Upset plots were made using custom code based on the R package UpSetR (Conway *et*
247 *al.* 2017), see Supplemental Methods. Community assembly processes contributing to the whole
248 bacterial communities' structure were accomplished using NTI calculations (Stegen *et al.* 2012,
249 2015; Dini-Andreote *et al.* 2015; Barnett *et al.* 2020; Ning *et al.* 2020), see Supplemental
250 Methods. βNTI values for site pairs within each fire classification were compared across these
251 classes using Kruskall-Wallis and *post hoc* pairwise Dunn tests. The relationship between βNTI
252 values for site pairs and differences in soil temperature, the difference in soil pH, and their
253 interaction were examined using a linear model after scaling and centering both factors to make
254 them directly comparable.
255
256 **Results**
257 *Soil temperature and pH vary over fire classification*
258 As expected, fire-affected soils were generally hotter than recovered and reference soils.
259 Notably, the fire-affected soil temperatures decreased over the seven years, yet no consistent
260 changes over time were observed in recovered or reference sites (Fig. 1B, Table S2; LME

261 models). This pattern was confirmed by daily temperatures in selected sites that were hourly
262 tracked over the seven years by the *in situ* HOBO monitors (Fig. S2). Soil pH did not change
263 over time (Fig. S3A, Table S2; LME models), though it did overall differ across fire
264 classifications (ANOVA: DF = 2, F = 14.54, p-value < 0.001). pH was lower in recovered sites
265 than either reference or fire-affected sites, and the pH range across fire-affected sites was large
266 (Fig. S3B, *post hoc* Tukey's: p-values < 0.05).
267
268 *Bacterial diversity changes across fire classification and over time*
269 Faith's phylogenetic diversity (PD) increased over time in fire-affected soils for both
270 whole communities and active subsets but no increase in recovered or reference soils (Fig. S4;
271 Table S3; LME models). When time and fire classification were ignored, PD increased as soil
272 temperature decreased for whole communities and active subsets (Fig. 1C and D, Table S4; LME
273 models). Overall bacterial and archaeal counts, as determined by qPCR, showed no significant
274 relationship to soil temperature across our soils (Table S5; LME model).
275 For whole bacterial communities, phylogenetic beta diversity (weighted UniFrac) was
276 explained by fire classification (18.0% variation explained), time (5.7%), and their interaction
277 (4.0%) (Fig. S5, Table S6; PERMANOVA). *Post hoc* tests within each fire class showed that
278 time was explanatory only in fire-affected sites (Fig S6, Table S7). While fire classification was
279 explanatory in all years, the variation explained (R^2) decreased between 2015 and 2018 (Fig. S7,
280 Table S7). Differences across fire classifications could be attributed to differences in beta-
281 dispersion (ANOVA; df = 2, F = 34.722, p-value < 0.001). Specifically, dispersion was higher
282 among fire-affected soils than recovered and reference soils (Table S8).

283 For the active subset of the community, fire classification (12.4% variation explained)
284 and time (5.7%), but not their interaction, explained phylogenetic beta diversity (Fig. S8, Table
285 S6; PERMANOVA). Beta-dispersion again varied across fire classifications for the active subset
286 (ANOVA; df = 2, F = 17.536, p-value < 0.001). Dispersion across fire-affected soil was higher
287 than recovered and reference soils, though the effect was smaller than for the whole community
288 (Table S8).
289 Measured edaphic factors, particularly soil temperature, pH, and pH-associated properties
290 (*e.g.,* Ca, Mg, and Fe concentration), explained a large portion of the variation in community
291 structure for both whole communities (Fig. S9A; variation explained = 45.342%) and active
292 subsets (Fig. S9B; variation explained = 35.789%). As expected, the variation between fire-
293 affected and both reference and recovered sites was largely associated with soil temperature. In
294 contrast, variation across and within the reference and recovered sites was primarily associated
295 with pH (Fig. S9).
296
297 *Disturbance intensity drives community trajectories*
298 For both the whole bacterial communities and active subsets, time-lag analysis showed
299 increasing community dissimilarity as the timespan between the samplings increases for fire-
300 affected sites but no relationship for either recovered or reference soils (LME models; Fig. 2A
301 and B, Table S9). The slopes of the time-lag relationships were positively correlated to the
302 maximum soil temperature of the sites (Fig 2C and D; linear regression; whole community: R^2 =
303 0.67, p-value < 0.001, active subset: R^2 = 0.30, p-value = 0.011). Notably, the relationship
304 between the time-lag slope and maximum soil temperature was stronger for the whole
305 community than the active subset.

306 For both the whole communities and active subsets, there was higher directionality in the
307 fire-affected sites than either recovered or reference sites, with no significant difference between
308 the latter classifications (Fig. 3A and B; Kruskal-Wallis rank sum test; whole community: chi-
309 squared = 9.04, df = 2, p-value = 0.01, active subset: chi-squared = 8.67, df = 2, p-value = 0.01;
310 *post hoc* Dunn's tests). Community directionality was positively correlated with maximum soil
311 temperature (a proxy for disturbance intensity), with, again, a stronger relationship for the whole
312 communities relative to the active subsets (Figs. 3C and D; linear regression; whole community:
313 $R^2 = 0.55$, p-value < 0.001, active subset: $R^2 = 0.20$, p-value = 0.036).
314 We next tested whether the change in community structure between disturbed soils (*i.e.,*
315 fire-affected and recovered soils) and reference soils within years changed over time or was
316 associated with soil temperature. We found that for both whole communities and active subsets,
317 disturbed communities tended to become more like the reference communities over time and as
318 temperature decreased (Fig. 3E-H; LME models). While fire-affected and recovered soils
319 demonstrated increased similarity to reference communities over time, the slope of the change in
320 community distances was higher for fire-affected communities than recovered communities (Fig
321 3E-F).
322
323 *Active members contribute little to shifts in the whole community*
324 Across most sites, less than 50% of the Bray-Curtis dissimilarity in the whole community
325 was attributable to active OTUs. For fire-affected sites, the dissimilarity attributed to active taxa
326 decreased as the period between sampling years increased (Fig. 4, Table S10; LME models; p-
327 values < 0.05). This trend was statistically supported when partitioning taxa as active at the

328 earlier and later time points in the year-pairing. In contrast, no such trend was observed for
329 recovered or reference sites.
330
331 *Interannual OTU activity dynamics vary across fire-affected and unaffected soils*
332 Many OTUs had distinctive yearly activity patterns (Fig. 5 and Figs. S10 and S11). For
333 fire-affected sites (Fig. 5A), most OTUs tended to have consistent activity in later sampling years
334 (*e.g.,* 2018-2021) but not earlier (*e.g.,* 2015-2017). This trend suggests that many OTUs became
335 active in later years for fire-affected sites, corresponding to cooling soil temperatures and
336 recovery. For reference and recovered soils (Fig. 5B), most OTUs had no clear annual
337 progression or delineation, suggesting more random activity patterns in these soils that
338 experienced ambient temperatures. Activity groups were taxonomically diverse for both cases,
339 with no obvious enrichment in taxa at the phylum level or *Proteobacteria* class.
340
341 *Community assembly processes for whole communities differ across fire classifications*
342 While the majority of within-year, site-to-site comparisons indicate dominance of
343 homogeneous selection ($\beta NTI < -2$), phylogenetic turnover among fire-affected sites tended to
344 be higher than among recovered or reference sites (Fig. 6A; Kruskal-Wallis rank sum test: DF =
345 2, chi-squared = 68.399, p-value < 0.001; post hoc Dunn test) with many site pairs demonstrating
346 weak selection ($-2 \leq \beta NTI \leq 2$) or variable selection ($\beta NTI > 2$). This pattern was consistent
347 across seven years (Fig. 6D and S12). For these site pairs with weak selection, homogenizing
348 dispersal ($RC_{bray} < -0.95$), followed by drift alone ($-0.95 \leq RC_{bray} \leq 0.95$), tended to be the
349 dominant assembly process (Fig. 6D). Scaled between-site differences in soil pH and
350 temperature were both positively associated with βNTI, but their interaction was not (Fig. 6B

351 and C, Table S11; linear regression: $R^2 = 0.5031$, p-value < 0.001). The coefficient for scaled
352 difference in pH (2.63) is much larger than that of scaled difference in temperature (0.42).
353

354 **Discussion**

355 We used long-term soil microbiome surveys from Centralia, Pennsylvania, USA, to
356 examine the resilience of whole bacterial communities and their active members impacted by
357 heat press disturbance from a subterranean coal seam fire. Over seven years, we observed
358 general cooling of the fire-affected sites, indicating a gradual reduction in disturbance intensity.
359 Cooling was not unexpected at these locations (Elick 2011). While heat intensity decreased in
360 most sites, other fire-induced environmental impacts continued, exemplified by elevated local
361 CO_2 concentrations and steam venting observed in some soils only a few degrees Celsius above
362 ambient temperature. The gradual change in disturbance intensity provided a unique opportunity
363 to observe the transition and recovery of the microbial communities during both early stages and
364 later stages of recovery (*i.e.,* cooling fire-affected and recovered sites, respectively). Temporal
365 trends in bacterial diversity revealed strong evidence for the resilience of the microbiomes in
366 both the whole communities and their active subsets. In comparison, communities in recovered
367 and reference sites were more stable over the years. These findings agree with our previous
368 study, which included soils compared along the fire-impact gradient within one sampling year,
369 that the whole bacterial communities in Centralia soils are resilient (Lee *et al.* 2017).

370 Dispersal is an important microbiome assembly mechanism for soil (Albright & Martiny
371 2018; Barnett *et al.* 2020; Evans *et al.* 2020; Walters *et al.* 2022). Across Centralia sites, when
372 selection was weak, homogenizing dispersal was the dominant assembly process. Dispersal
373 likely explains the increased alpha diversity observed as fire-affected soils cool. However, even

374 when dispersal is high, immigrant taxa may not necessarily be immediately active or later
375 become established. Rather, their DNA may remain extractable either in intact cells (dormant or
376 dead) or as extracellular DNA (Morrissey *et al.* 2015; Carini *et al.* 2017; Lennon *et al.* 2018).
377 The microbial conveyor belt hypothesis proposes that dormancy aids microbial dispersal
378 capability (Mestre & Höfer 2021), though more supporting evidence is needed (Choudoir &
379 DeAngelis 2022). During a 45-week mesocosm experiment with soil from Centralia reference
380 sites that explicitly controlled dispersal (Sorensen & Shade 2020), we observed that post-
381 disturbance activation of dispersed taxa contributed to overall resilience. Building from these
382 collective results, we present an updated working hypothesis to integrate dispersal and dormancy
383 mechanisms in soil microbiome resilience. We hypothesize that dispersed members from the
384 regional species pool progressively replace taxa lost to disturbance as thermal selection weakens,
385 but some likely maintain dormancy while conditions remain suboptimal. This process effectively
386 rebuilds and accumulates the dormant "seed bank" but does not contribute immediately to
387 functional recovery (*i.e.,* active populations) until conditions become favorable for activity.
388 Thus, re-establishing the microbial seed bank during or after a disturbance could provide a
389 restoration management strategy (Moreira-Grez *et al.* 2019; King & Bell 2022; Shade 2023).
390 Patterns of OTU activity over time in fire-affected sites demonstrated that many bacteria
391 are likely to be activating (either after dispersal or from the local seed bank) in the fire-affected
392 soils over the last few years as the soils have cooled. Of the top 20 interannual activity patterns,
393 most taxa tended to have observed activity only in the later sampling years. In other words, many
394 active taxa become detectably active after one to three years of no detectable activity in fire-
395 affected soil. This is best exemplified by the second most numerous activity pattern that includes
396 activity detected in 2016-2021 but not 2015, possibly suggesting significant activation of taxa

397 after this first sampling year in particular. In reference and recovered sites, the top 20 patterns
398 exhibited random years in which no activity is detected, including patterns with detectable
399 activity in the first few sampling years. We further see that the most numerous activity patterns
400 include many phyla, suggesting that activation and perhaps recovery of the active community
401 subset is phylogenetically indiscriminate at high taxonomic levels.

402 Notably, the temporal changes within the whole communities were greater than in their
403 active subsets, indicating differences in perceived resilience and recovery between the active and
404 whole communities. For example, time explains more variation in beta diversity for whole
405 communities than for active subsets, and no interaction was found between time and fire
406 classification for active communities. Similarly, the relationships between maximum temperature
407 and both time lag slopes and trajectory directionality were weaker for active subsets than the
408 whole communities. When considering variation in the whole community structure within a site
409 over time, active OTUs tended to explain a smaller percentage of the community dissimilarity as
410 the timescale increased, but only for fire-affected sites. This important finding indicates that over
411 multiple years, changes in the structure of the active subset account for less of the change in
412 overall community structure in recovering soils. Thus, we propose that while the overall bacterial
413 community is largely resilient, the active populations collectively may recover slower. This
414 conclusion refutes our original hypothesis that bacterial community resilience is largely
415 attributable to the dynamics of active populations. It suggests that dispersal enables bacterial taxa
416 from undisturbed soils to arrive and persist in the fire-affected soils as they cool, with some
417 immigrants remaining dormant though persistent as disturbance intensity slowly wanes. This
418 accumulation of inactive microbial diversity throughout a disturbance may enable recovery of
419 the bacterial community after the disturbance; this should be investigated in future studies.

420 pH and associated edaphic properties are well-known drivers of bacterial community
421 diversity and soil assembly (Fierer & Jackson 2006; Malik *et al.* 2017; Tripathi *et al.* 2018;
422 Barnett *et al.* 2020; Yavitt *et al.* 2020). Many pH related properties explained structural
423 differences among Centralia communities (e.g., Ca, Mg, Fe, etc.) and βNTI (Stegen *et al.* 2012,
424 2015) correlated to difference in soil pH, together indicating pH-related selection across
425 Centralia soils. βNTI also correlated to difference in soil temperature, though this relationship
426 was weaker than that of soil pH, and there was no statistically significant interaction between
427 these factors. We thus propose that while soil pH selection acts upon Centralia soil bacterial
428 communities, soil heating imposes either alternate selection pressures or increased stochasticity.
429 Soil acidification may be a legacy effect of mining (Rice & Herman 2012; Wang *et al.* 2020) or
430 coal fires in this area (Tobin-Janzen *et al.* 2005; Janzen & Tobin-Janzen 2008; Lee *et al.* 2017)
431 and may promote alternative stable states among the recovered communities distinct from
432 unaffected soils (Quadros *et al.* 2016).
433 Other mechanisms may also have contributed to the patterns we observed. First, cyclical
434 seasonal disturbance intensity patterns, as observed from HOBO temperature monitors, may
435 produce temporary conditions suitable for the growth or maintenance of fire-sensitive
436 populations (Philippot *et al.* 2021). Second, as soils are extremely diverse (Rondon *et al.* 1999),
437 the non-detection of rare taxa is a distinct possibility despite our deep sequencing, as
438 demonstrated by the rarefaction curves. Third, extracellular DNA (eDNA) may contribute to the
439 divergence in the whole community and active subset dynamics between fire-affected and
440 unheated soils because eDNA in soil degrades more rapidly at higher temperatures (Sirois &
441 Buckley 2018). However, a large influence of eDNA on the observed interannual patterns is not
442 expected due to the short lifespan of nucleic acids in soils in general.

Broadly, our findings and working conceptual model for bacterial community recovery from press disturbance have implications for understanding ecosystem recovery to large, long-term stress. We interpret the observed relatively high resilience of the whole community with somewhat lower resilience of the active subset to indicate that, while microbial community functional potential may recover rapidly along with the demographic recovery of members lost to the disturbance, the realized activity of these communities may take longer to recover because it is harbored within the dormant pool. As only the active subset of the community performs ecosystem functions and services, it is likely that biologically mediated soil processes, such as biogeochemical cycling, may remain altered for some period after disturbance intensity wanes, especially for functions with low redundancy among populations. If ecosystem function is used to measure ecosystem recovery (Harris 2003), then whole bacterial community surveys will provide a biased view of the recovery progress. However, our findings provide a positive outlook on the recovery potential of disturbed soils. Understanding the stability and potential for recovery of microbial communities will help to predict changes to vital ecosystem functions and develop methods of microbiome restoration.

Acknowledgments

We thank Tammy Tobin-Janzen for Centralia research consultation and local sampling support and Keara L Grady for coordinating fieldwork logistics and organization of multi-year soil procurement and processing. We additionally thank SH Lee, JW Sorensen, TK Dunivin, JL Chodkowski, N Stopnisek, and M Mechan Llontop for collecting samples. This work was supported by the U.S. National Science Foundation CAREER award #1749544 to AS. AS

acknowledges the French Centre National de la Recherche Scientifique (CNRS) support. We declare no conflicts of interest.

References

Aanderud, Z.T., Jones, S.E., Fierer, N. & Lennon, J.T. (2015). Resuscitation of the rare biosphere contributes to pulses of ecosystem activity. *Front. Microbiol.*, 6, 24.

Albright, M.B.N. & Martiny, J.B.H. (2018). Dispersal alters bacterial diversity and composition in a natural community. *ISME J.*, 12, 296–299.

Allison, S.D. & Martiny, J.B.H. (2008). Resistance, resilience, and redundancy in microbial communities. *Proc. Natl. Acad. Sci.*, 105, 11512–11519.

Barnett, S.E., Youngblut, N.D. & Buckley, D.H. (2020). Soil characteristics and land-use drive bacterial community assembly patterns. *FEMS Microbiol. Ecol.*, 96, fiz194.

Beisner, B.E., Haydon, D.T. & Cuddington, K. (2003). Alternative stable states in ecology. *Front. Ecol. Environ.*, 1, 376–382.

Blagodatskaya, E. & Kuzyakov, Y. (2013). Active microorganisms in soil: Critical review of estimation criteria and approaches. *Soil Biol. Biochem.*, 67, 192–211.

Blazewicz, S.J., Barnard, R.L., Daly, R.A. & Firestone, M.K. (2013). Evaluating rRNA as an indicator of microbial activity in environmental communities: limitations and uses. *ISME J.*, 7, 2061–2068.

Bowsher, A.W., Kearns, P.J. & Ashley, S. (2019). 16S rRNA/rRNA Gene Ratios and Cell Activity Staining Reveal Consistent Patterns of Microbial Activity in Plant-Associated Soil. *mSystems*, 4, e00003-19.

De Cáceres, M., Coll, L., Legendre, P., Allen, R.B., Wiser, S.K., Fortin, M.-J., *et al.* (2019). Trajectory analysis in community ecology. *Ecol. Monogr.*, 89, e01350.

Carini, P., Marsden, P.J., Leff, J.W., Morgan, E.E., Strickland, M.S. & Fierer, N. (2017). Relic DNA is abundant in soil and obscures estimates of soil microbial diversity. *Nat. Microbiol.*,

2, 16242.

Choudoir, M.J. & DeAngelis, K.M. (2022). A framework for integrating microbial dispersal modes into soil ecosystem ecology. *iScience*, 25, 103887.

Colovas, J., Bintarti, A.F., Mechan Llontop, M.E., Grady, K.L. & Shade, A. (2022). Do-it-Yourself Mock Community Standard for Multi-Step Assessment of Microbiome Protocols. *Curr. Protoc.*, 2, e533.

Conway, J.R., Lex, A. & Gehlenborg, N. (2017). UpSetR: an R package for the visualization of intersecting sets and their properties. *Bioinformatics*, 33, 2938–2940.

Dini-Andreote, F., Stegen, J.C., van Elsas, J.D. & Salles, J.F. (2015). Disentangling mechanisms that mediate the balance between stochastic and deterministic processes in microbial succession. *Proc. Natl. Acad. Sci.*, 112, E1326 LP-E1332.

Elick, J.M. (2011). Mapping the coal fire at Centralia, Pa using thermal infrared imagery. *Int. J. Coal Geol.*, 87, 197–203.

Evans, S.E., Bell-Dereske, L.P., Dougherty, K.M. & Kittredge, H.A. (2020). Dispersal alters soil microbial community response to drought. *Environ. Microbiol.*, 22, 905–916.

Fierer, N. & Jackson, R.B. (2006). The diversity and biogeography of soil bacterial communities. *Proc. Natl. Acad. Sci.*, 103, 626–631.

Glassman, S.I. & Martiny, J.B.H. (2018). Broadscale Ecological Patterns Are Robust to Use of Exact Sequence Variants versus Operational Taxonomic Units. *mSphere*, 3, e00148-18.

Griffiths, B.S. & Philippot, L. (2013). Insights into the resistance and resilience of the soil microbial community. *FEMS Microbiol. Rev.*, 37, 112–129.

Griffiths, R.I., Whiteley, A.S., O'Donnell, A.G. & Bailey, M.J. (2000). Rapid Method for Coextraction of DNA and RNA from Natural Environments for Analysis of Ribosomal

DNA- and rRNA-Based Microbial Community Composition. *Appl. Environ. Microbiol.*, 66, 5488–5491.

Harris, J.A. (2003). Measurements of the soil microbial community for estimating the success of restoration. *Eur. J. Soil Sci.*, 54, 801–808.

Holling, C.S. (1996). Engineering Resilience versus Ecological Resilience. In: *Engineering within Ecological Constraints* (ed. Schulze, P.). National Academy Press, Washington, D.C., pp. 31–43.

Janzen, C. & Tobin-Janzen, T. (2008). Microbial Communities in Fire-Affected Soils. In: *Microbiology of Extreme Soils* (eds. Dion, P. & Nautiyal, C.S.). Springer Berlin Heidelberg, Berlin, Heidelberg, pp. 299–316.

Jones, S.E. & Lennon, J.T. (2010). Dormancy contributes to the maintenance of microbial diversity. *Proc. Natl. Acad. Sci.*, 107, 5881 LP – 5886.

Kearns, P.J. & Shade, A. (2018). Trait-based patterns of microbial dynamics in dormancy potential and heterotrophic strategy: case studies of resource-based and post-press succession. *ISME J.*, 12, 2575–2581.

King, W.L. & Bell, T.H. (2022). Can dispersal be leveraged to improve microbial inoculant success? *Trends Biotechnol.*, 40, 12–21.

Lamothe, K.A., Somers, K.M. & Jackson, D.A. (2019). Linking the ball-and-cup analogy and ordination trajectories to describe ecosystem stability, resistance, and resilience. *Ecosphere*, 10, e02629.

Lee, S.-H., Sorensen, J.W., Grady, K.L., Tobin, T.C. & Shade, A. (2017). Divergent extremes but convergent recovery of bacterial and archaeal soil communities to an ongoing subterranean coal mine fire. *ISME J.*, 11, 1447–1459.

536 Lennon, J.T. & Jones, S.E. (2011). Microbial seed banks: the ecological and evolutionary
537 implications of dormancy. *Nat. Rev. Microbiol.*, 9, 119–130.
538 Lennon, J.T., Muscarella, M.E., Placella, S.A. & Lehmkuhl, B.K. (2018). How, when, and where
539 relic DNA affects microbial diversity. *MBio*, 9, e00637-18.
540 Madsen, E.L. (2011). Microorganisms and their roles in fundamental biogeochemical cycles.
541 *Curr. Opin. Biotechnol.*, 22, 456–464.
542 Malik, A.A., Thomson, B.C., Whiteley, A.S., Bailey, M. & Griffiths, R.I. (2017). Bacterial
543 Physiological Adaptations to Contrasting Edaphic Conditions Identified Using Landscape
544 Scale Metagenomics. *MBio*, 8, e00799-17.
545 McMurdie, P.J. & Holmes, S. (2013). phyloseq: An R package for reproducible interactive
546 analysis and graphics of microbiome census data. *PLoS One*, 8, e61217.
547 Mendes, R., Garbeva, P. & Raaijmakers, J.M. (2013). The rhizosphere microbiome: significance
548 of plant beneficial, plant pathogenic, and human pathogenic microorganisms. *FEMS*
549 *Microbiol. Rev.*, 37, 634–663.
550 Mestre, M. & Höfer, J. (2021). The Microbial Conveyor Belt: Connecting the Globe through
551 Dispersion and Dormancy. *Trends Microbiol.*, 29, 482–492.
552 Moreira-Grez, B., Muñoz-Rojas, M., Kariman, K., Storer, P., O'Donnell, A.G., Kumaresan, D.,
553 *et al.* (2019). Reconditioning Degraded Mine Site Soils With Exogenous Soil Microbes:
554 Plant Fitness and Soil Microbiome Outcomes. *Front. Microbiol.*, 10, 1617.
555 Morrissey, E.M., McHugh, T.A., Preteska, L., Hayer, M., Dijkstra, P., Hungate, B.A., *et al.*
556 (2015). Dynamics of extracellular DNA decomposition and bacterial community
557 composition in soil. *Soil Biol. Biochem.*, 86, 42–49.
558 Nemergut, D.R., Stanish, L.F., Schmidt, S.K., Ferrenberg, S., Lynch, R.C., Wickey, P., *et al.*

(2013). Patterns and Processes of Microbial Community Assembly. *Microbiol. Mol. Biol. Rev.*, 77, 342–356.

Ning, D., Yuan, M., Wu, L., Zhang, Y., Guo, X., Zhou, X., *et al.* (2020). A quantitative framework reveals ecological drivers of grassland microbial community assembly in response to warming. *Nat. Commun.*, 11, 4717.

Oksanen, J., Blanchet, F.G., Friendly, M., Kindt, R., Legendre, P., McGlinn, D., *et al.* (2018). vegan: Community Ecology Package.

Philippot, L., Griffiths, B.S. & Langenheder, S. (2021). Microbial Community Resilience across Ecosystems and Multiple Disturbances. *Microbiol. Mol. Biol. Rev.*, 85, e00026-20.

Pimm, S.L. (1984). The complexity and stability of ecosystems. *Nature*, 307, 321–326.

Pinheiro, J., Bates, D., DebRoy, S., Sarkar, D. & R Core Team. (2020). nlme: Linear and Nonlinear Mixed Effects Models.

Quadros, P.D. de, Zhalnina, K., Davis-Richardson, A.G., Drew, J.C., Menezes, F.B., Camargo, F.A. d. O., *et al.* (2016). Coal mining practices reduce the microbial biomass, richness and diversity of soil. *Appl. Soil Ecol.*, 98, 195–203.

R Core Team. (2018). R: A language and environment for statistical computing.

Rice, K.C. & Herman, J.S. (2012). Acidification of Earth: An assessment across mechanisms and scales. *Appl. Geochemistry*, 27, 1–14.

Rondon, M.R., Goodman, R.M. & Handelsman, J. (1999). The Earth's bounty: assessing and accessing soil microbial diversity. *Trends Biotechnol.*, 17, 403–409.

Schloss, P.D. (2021). Amplicon Sequence Variants Artificially Split Bacterial Genomes into Separate Clusters. *mSphere*, 6, e00191-21.

Shade, A. (2018). Understanding Microbiome Stability in a Changing World. *mSystems*, 3,

e00157-17.

Shade, A. (2023). Microbiome rescue: directing resilience of environmental microbial communities. *Curr. Opin. Microbiol.*, 72, 102263.

Shade, A., Jones, S.E., Caporaso, J.G., Handelsman, J., Knight, R., Fierer, N., *et al.* (2014). Conditionally Rare Taxa Disproportionately Contribute to Temporal Changes in Microbial Diversity. *MBio*, 5, e01371-14.

Shade, A., Peter, H., Allison, S., Baho, D., Berga, M., Buergmann, H., *et al.* (2012). Fundamentals of Microbial Community Resistance and Resilience. *Front. Microbiol.*, 3, 417.

Sirois, S.H. & Buckley, D.H. (2018). Factors governing extracellular DNA degradation dynamics in soil. *Environ. Microbiol. Rep.*, 11, 173–184.

Sorensen, J.W. & Shade, A. (2020). Dormancy dynamics and dispersal contribute to soil microbiome resilience. *Philos. Trans. R. Soc. B Biol. Sci.*, 375, 20190255.

Stegen, J.C., Lin, X., Fredrickson, J.K. & Konopka, A.E. (2015). Estimating and mapping ecological processes influencing microbial community assembly. *Front. Microbiol.*, 6, 370.

Stegen, J.C., Lin, X., Konopka, A.E. & Fredrickson, J.K. (2012). Stochastic and deterministic assembly processes in subsurface microbial communities. *ISME J.*, 6, 1653–1664.

Sturbois, A., De Cáceres, M., Sánchez-Pinillos, M., Schaal, G., Gauthier, O., Mao, P. Le, *et al.* (2021). Extending community trajectory analysis: New metrics and representation. *Ecol. Modell.*, 440, 109400.

Tobin-Janzen, T., Shade, A., Marshall, L., Torres, K., Beblo, C., Janzen, C., *et al.* (2005). Nitrogen changes and domain Bacteria ribotype diversity in soils overlaying the Centralia, Pennsylvania underground coal mine fire. *Soil Sci.*, 170.

605 Tripathi, B.M., Stegen, J.C., Kim, M., Dong, K., Adams, J.M. & Lee, Y.K. (2018). Soil pH
606 mediates the balance between stochastic and deterministic assembly of bacteria. *ISME J.*,
607 12, 1072–1083.
608 Turner, T.R., James, E.K. & Poole, P.S. (2013). The plant microbiome. *Genome Biol.*, 14, 209.
609 Vellend, M. (2010). Conceptual Synthesis in Community Ecology. *Q. Rev. Biol.*, 85, 183–206.
610 Walters, K.E., Capocchi, J.K., Albright, M.B.N., Hao, Z., Brodie, E.L. & Martiny, J.B.H. (2022).
611 Routes and rates of bacterial dispersal impact surface soil microbiome composition and
612 functioning. *ISME J.*, 16, 2295–2304.
613 Wang, H., Zhang, J., Zhang, L., Wang, J. & Xu, Z. (2020). Gas Emission and Soil Chemical
614 Properties Associated with Underground Coal Fires, Wuda Coalfield, Inner Mongolia,
615 China. *Nat. Resour. Res.*, 29, 3973–3985.
616 Yavitt, J.B., Roco, C.A., Debenport, S.J., Barnett, S.E. & Shapleigh, J.P. (2020). Community
617 Organization and Metagenomics of Bacterial Assemblages Across Local Scale pH
618 Gradients in Northern Forest Soils. *Microb. Ecol.*, 81, 758–769.
619
620

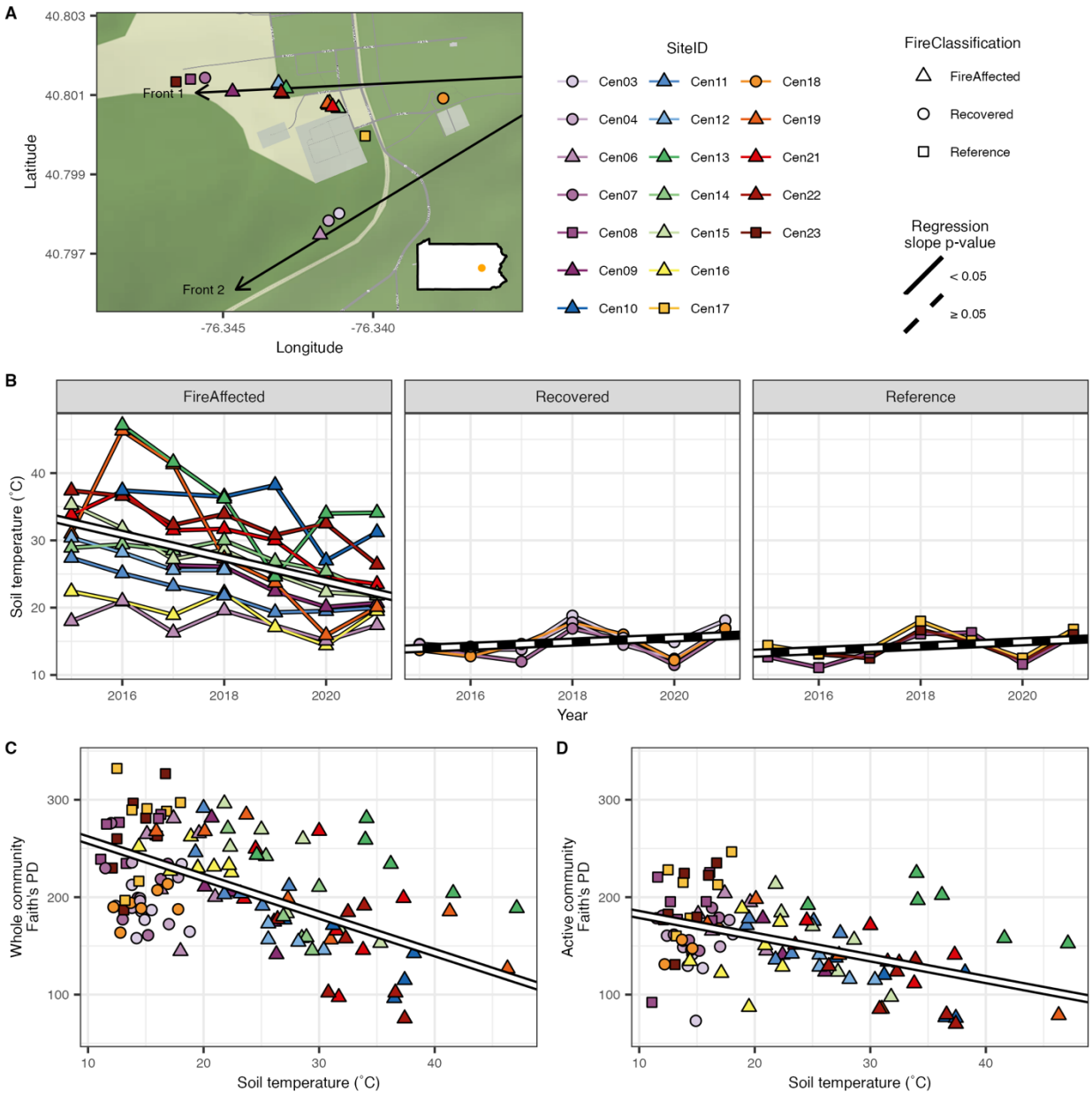

Figure 1: In the fire-affected sites, soils cooled over time, and along with this cooling, bacterial alpha diversity increased. A) Map of collection sites in Centralia, Pennsylvania, USA. B) Tracking of soil temperature (˚C) over the seven sampling years for each site showed general soil cooling in fire-affected sites. C) The bacterial community's phylogenetic diversity (Faith's PD) decreased as soil core temperature increased. D) Active bacterial community subset phylogenetic diversity decreased as soil core temperature increased. For all plots, colored points and lines indicate site and fire classification. For plots B-D, white and black lines indicate linear mixed-effects regressions using site ID as the random effect, with solid white lines indicating statistically significant slopes (p-value < 0.05) and dashed lines indicating non-statistical significance (p-value ≥ 0.05). Full statistics are found in tables S2-S4, and phylogenetic diversity trends over time are found in Fig. S4.

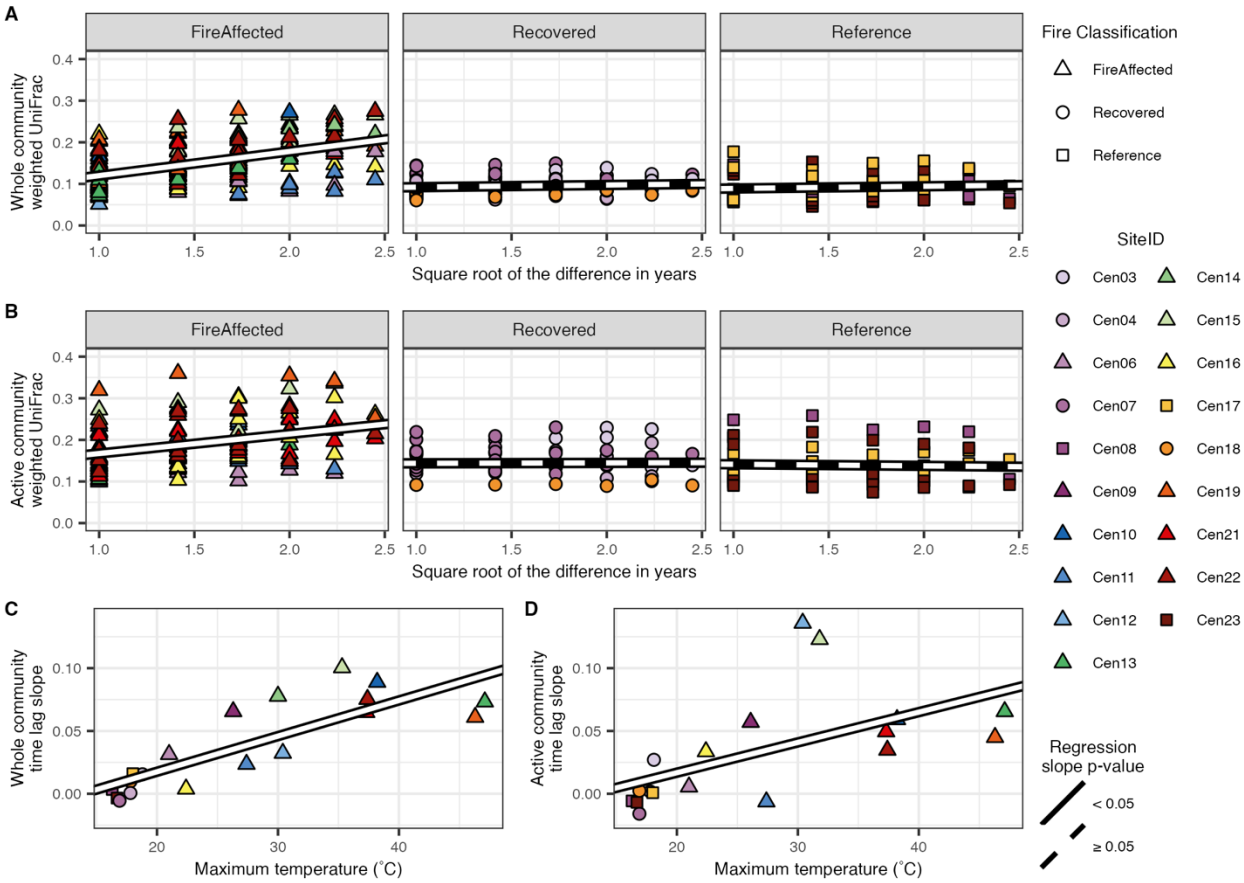

Figure 2: Time-lag analysis demonstrated that variation in the whole bacterial community and active subset structure between samplings of the same site increased as the time difference between sampling increased. However, this trend was only statically significant for fire-affected sites. A) Whole community time-lag analysis. B) Active community subset time-lag analysis. C) Slopes of whole community time-lag regressions made individually for sites increased as maximum soil temperature (proxy of disturbance intensity) increased across sites. D) Slopes of active community subset time-lag regressions made individually for sites increased as maximum soil temperature increased across sites. Points indicate site ID and fire classification. White and black lines indicate linear mixed-effects regressions using site ID as the random effect (A and B) and linear regression (C and D) with solid white lines indicating statistically significant slopes (p-value < 0.05) and dashed lines indicating non-statistical significance (p-value ≥ 0.05). Full statistics for the linear mixed effects regressions are provided in Table S8.

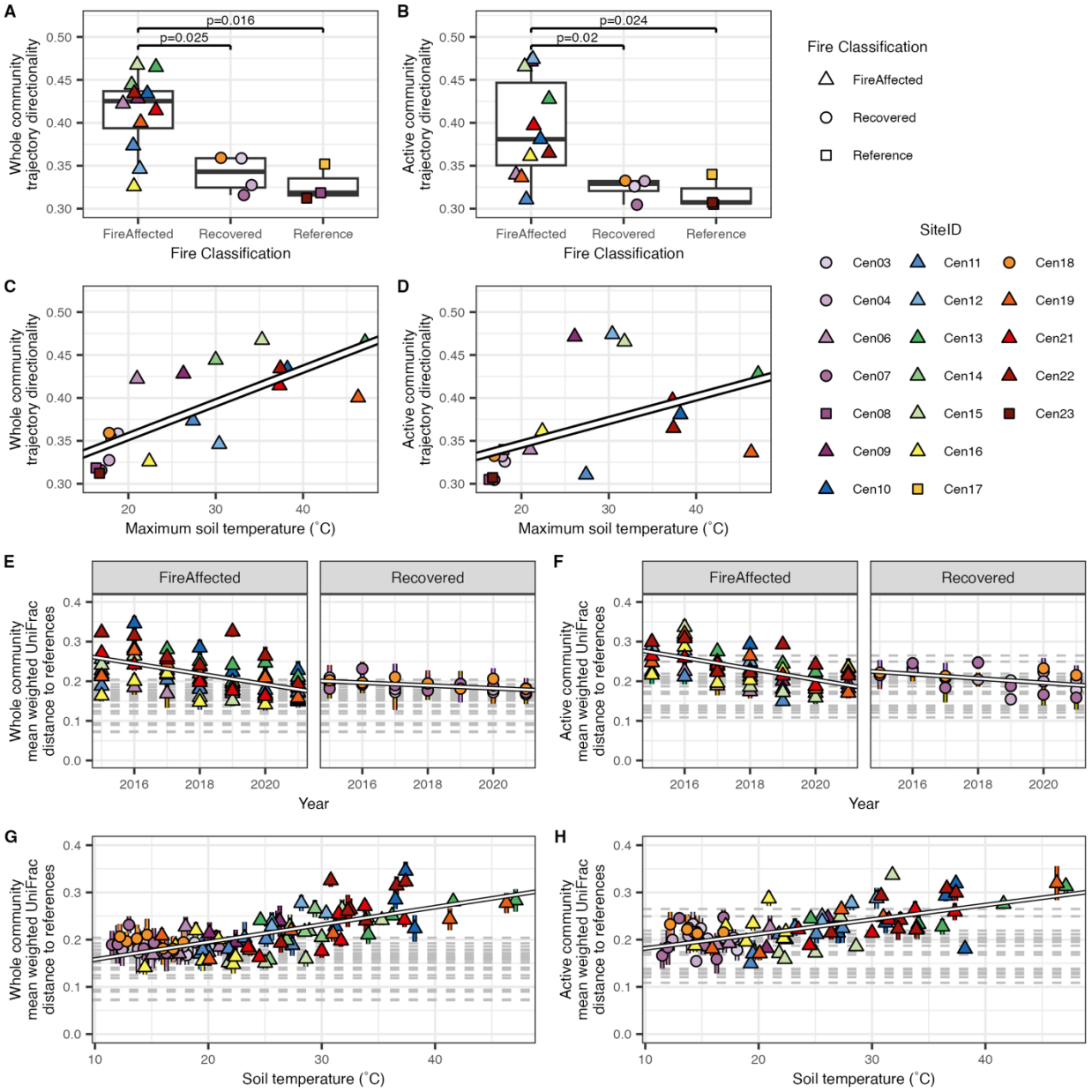

Figure 3: Trajectory analysis demonstrated that directionality in both whole bacterial community (A) and active subset (B) structural shifts over time were generally highest in fire-affected soils compared to recovered and reference soils. Post-hoc pairwise Dunn's test p-values < 0.05 are displayed above statistical significance indicator bars. Directionality in both whole bacterial community (C) and active subset (D) structural shifts increased as maximum soil temperature within sites increased. For both whole bacterial communities and active subsets, disturbed soil communities became more structurally similar to the undisturbed reference communities over time as soils cooled (E and F, respectively) and soils cooled (G and H respectively). Structural dissimilarity was calculated as the mean weighted UniFrac distance between fire-affected and recovered sites and the three reference sites paired within the sampling year. White lines indicate linear regressions (C and D) and linear mixed-effects regressions using site ID as the random effect (E-H), which had statistically significant slopes (p-value < 0.05). For

figures A-D, points indicate all samples' site ID and fire classification. For figures E-H, points indicate the site ID and fire classification (fire affected or recovered) of the disturbed site with error bars representing the standard error for the distance between the sample and the three paired reference samples from the same year. For E-H, grey dashed horizontal lines indicate community distances between the reference sites within each year.

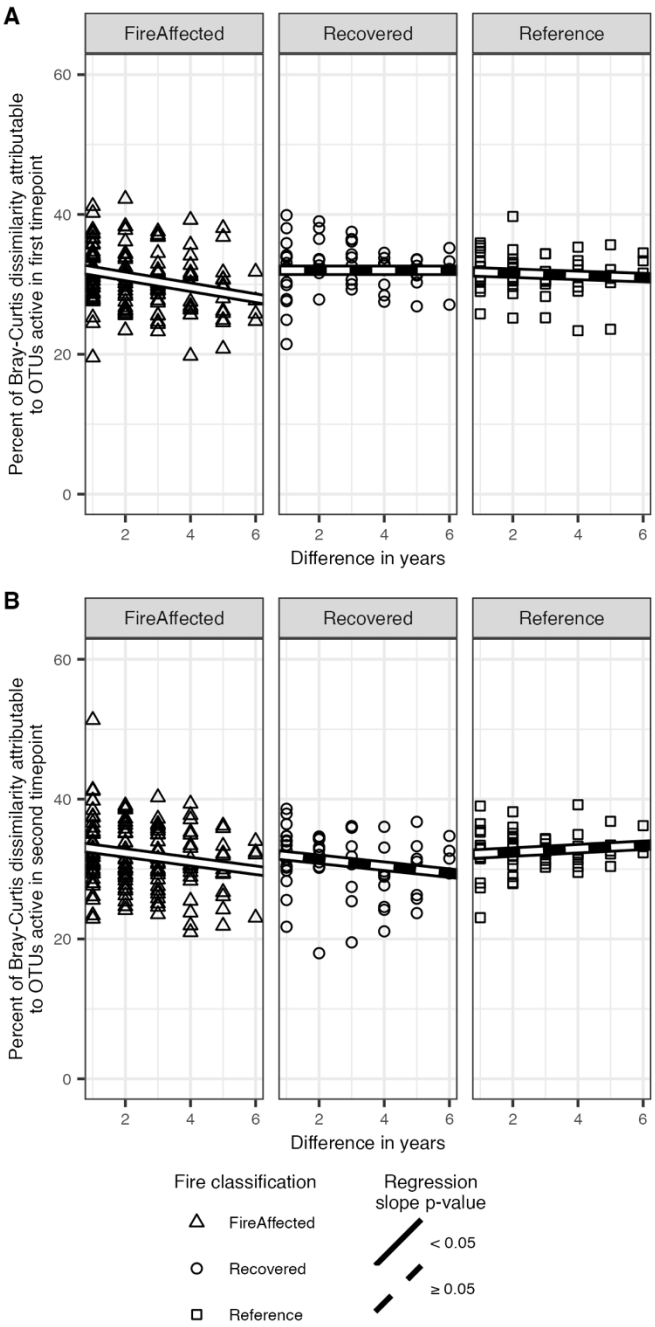

Figure 4: For fire-affected sites, the whole bacterial community structural dissimilarity attributable to the active subset decreases as the time between sampling time points increases. In

other words, less of the whole community dissimilarity is attributable to the active subset across larger timescales for fire-affected sites but not for recovered or reference sites. This holds across site pairs for OTUs active in (A) the early timepoint (*e.g.,* 2016 when comparing 2016 and 2020) and in (B) the later timepoint (*e.g.,* 2020 when comparing 2016 and 2020). Bray-Curtis dissimilarity within a site was used to partition OTUs active in either each pair's early or late time points. White and black lines indicate linear mixed-effects regressions using site ID as the random effect, with solid white lines indicating statistically significant slopes (p-value < 0.05) and dashed lines indicating non-statistical significance (p-value ≥ 0.05).

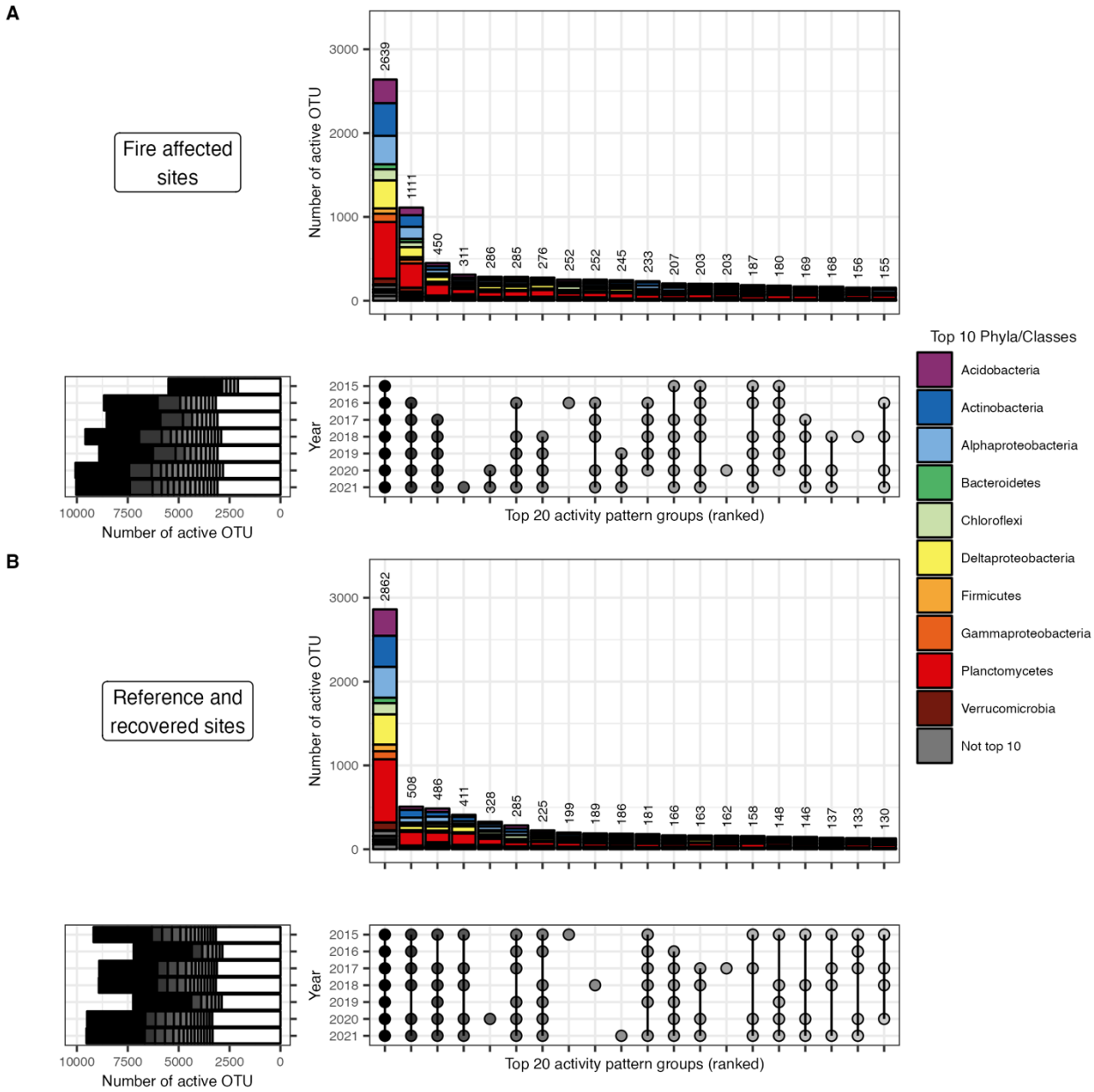

Figure 5: UpSet plots of the top 20 (as determined by OTU count) observed activity dynamics across years for (A) fire-affected sites and (B) combined recovered and reference sites. All sites

691 sampled each year were combined such that OTUs were defined as active if they had an RNA:
692 DNA ≥ 1 in at least one site within that year. The bottom right plots show the activity patterns of
693 the top 20 groups, with dots indicating activity within that year and groups ordered by OTU
694 membership. The top vertical bar chart shows the number of OTUs within each activity group,
695 colored by the top 10 phyla (class for *Proteobacteria*). The bottom left horizontal bar chart
696 shows the number of active OTUs within each year, colored by their membership in the top 20
697 activity groups. White sections of the bars indicate OTUs from the other 107 groups (see Figs.
698 S10 and S11 for all 127 activity groups). For the fire-affected sites (A), most of the top 20
699 activity groups do not have detectable activity in the first few sampled years, while most of the
700 top 20 activity groups for reference and recovered sites (B) have detectable activity during those
701 years.
702
703
704

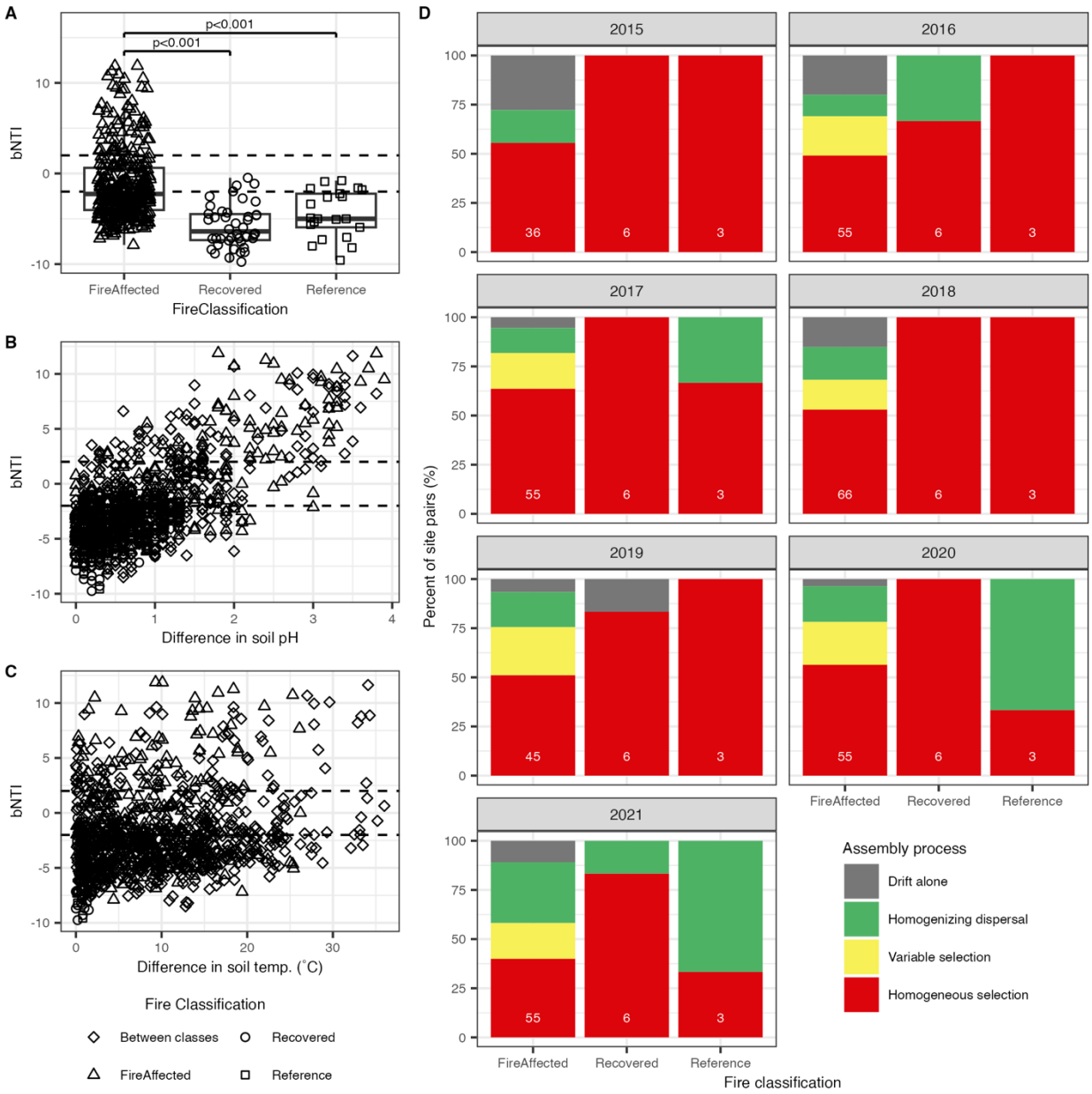

Figure 6: The whole bacterial community assembly dynamics across sites were measured with standardized phylogenetic and structural turnover. A) βNTI is generally higher between fire-affected sites than recovered or reference sites whose site pairs almost always have a βNTI < 2, indicating homogeneous selection. Post hoc pairwise Dunn's test p-values < 0.05 are displayed above statistical significance indicator bars. B) Regardless of fire classification, βNTI tended to increase as the difference in soil pH between sites increased, indicating pH-related selection pressures in these soils. C) Regardless of fire classification, βNTI tended to increase as the difference in soil temperature between sites increased, indicating some temperature-related selection pressures in these soils. Linear regressions, including these two relationships and their interaction, are provided in Table S10. D) Percentage of site pairs within each fire classification and year for which community assembly can be attributed to the five assembly processes

718 examined with βNTI and RC_{bray}. The numbers of site pairs are indicated by white numbers at the
719 bottom of each bar. All site pairs were within each year, not across years.